catalysts

MDPI

Communication

Copper Oxide Nanoparticles over Hierarchical Silica Monoliths for Continuous-Flow Selective Alcoholysis of Styrene Oxide

Marcello Marelli [1], Federica Zaccheria [2], Nicoletta Ravasio [2], Emanuela Pitzalis [3], Youcef Didi [4], Anne Galarneau [4], Nicola Scotti [1,*] and Claudio Evangelisti [3,*]

[1] CNR-Istituto di Scienze e Tecnologie Chimiche "Giulio Natta" (SCITEC), Via Fantoli 16/15, 20133 Milano, Italy
[2] CNR-Istituto di Scienze e Tecnologie Chimiche "Giulio Natta" (SCITEC), Via Golgi 19, 20133 Milano, Italy
[3] CNR-Istituto di Chimica dei Composti Organometallici (ICCOM), Via G. Moruzzi 1, 56124 Pisa, Italy
[4] Institut Charles Gerhardt Montpellier (ICGM), University Montpellier, CNRS, ENSCM, F-34293 Montpellier, France
* Correspondence: nicola.scotti@scitec.cnr.it (N.S.); claudio.evangelisti@cnr.it (C.E.)

Abstract: A simple and reproducible approach for the synthesis of Cu-based heterogeneous catalysts, named flow chemisorption hydrolysis (flow-CH), is reported. The approach, derived from the CH method, allows size-controlled CuO nanoparticles (mean diameter 2.9 nm) to be obtained, that are highly and homogeneously dispersed into hierarchically meso-/macroporous silica monoliths. The Cu-based monolithic catalysts (CuO@SiO_2-MN, 8.4 wt.% Cu) were studied in the styrene oxide ring opening reaction at 60 °C in the presence of isopropanol, under continuous flow-through conditions. A remarkable activity with a steady-state conversion of 97% for 13 h and 100% selectivity towards the corresponding β-alkoxyalcohol was observed. The performances of CuO@SiO_2-MN were higher than those obtained in batch conditions with the previously reported CuO/SiO_2 catalysts and with the ground CuO@SiO_2-MN monolith in terms of productivity and selectivity. Moreover, a negligible Cu leaching (<0.6 wt.%) in reaction medium was observed. After 13 h CuO@SiO_2-MN catalysts could be regenerated by a mild calcination (220 °C) permitting reuse.

Keywords: Cu nanoparticles; silica monolith; continuous-flow; styrene alcoholysis

Citation: Marelli, M.; Zaccheria, F.; Ravasio, N.; Pitzalis, E.; Didi, Y.; Galarneau, A.; Scotti, N.; Evangelisti, C. Copper Oxide Nanoparticles over Hierarchical Silica Monoliths for Continuous-Flow Selective Alcoholysis of Styrene Oxide. *Catalysts* **2023**, *13*, 341. https://doi.org/10.3390/catal13020341

Academic Editor: Diego Luna

Received: 22 December 2022
Revised: 26 January 2023
Accepted: 1 February 2023
Published: 3 February 2023

1. Introduction

Continuous flow microreactors show a huge potential in organic synthesis over conventional batch ones for the development of green and sustainable synthetic processes leading to fine chemicals, including active pharmaceutical ingredients, agrochemicals and polymers [1–3]. Among the different approaches used to carry out heterogeneous catalysis in microfluidic devices (e.g., packed-bed, monolithic, wash coated reactors), the use of porous monoliths has received a great deal of attention in the last decade, because of the peculiar porous networks on a multilevel length scale that confer unique properties to these materials [4–7]. Indeed, the macro- and mesopores of monoliths ensure high surface areas and pores volumes and the macroporous network improves heat and mass transfer, allowing fine control of contact time between the substrate and the catalytically active site, as well as its accessibility [8]. Organic polymers were the first materials to demonstrate the advantages of the use of monoliths for catalytic continuous-flow production of fine chemicals [9]. However, polymeric monoliths suffer from limited thermal, mechanical, and chemical stability. On the other hand, silica monoliths featuring a homogeneous and isotropic network have been recently investigated as supports for continuous-flow catalytic processes, because of their mechanical and chemical stability imparting better resistance and rigidity under reaction conditions [10,11]. These particular silica monoliths with outstanding mass transfer properties are obtained by a combination of a sol-gel process and a spinodal decomposition, thanks to the presence of polymers such as polyethylene

oxide (PEO). The macropores are fully interconnected and feature a narrow pore size distribution, adjustable between 2 to 35 μm depending on PEO length and EO/Si ratio [12]. Their permeability is proportional to the inverse of the square of the macropore diameter, which allows the prediction of the pressure drop in continuous-flow processes [13]. The mesopores are created by a basic (NH_3 aqueous solution) post-treatment, transforming oligomeric silica species into silica nanoparticles (NPs) by Ostwald ripening. The mesopore diameters (in between silica NPs) are adjustable between 8 to 20 nm depending on the basic post-treatment duration, temperature and NH_3 aqueous solution concentration [13]. The specific surface area is inversely proportional to the mesopore diameter and ranges from 100 to 900 m^2/g. Moreover, the well-known easy functionalization of the silica surface allows the immobilization of catalytic species like organometallic complexes, enzymes, MOF (e.g., CuBTC), or metal nanoparticles in order to tailor their catalytic properties [13–21]. Particularly, noble metal nanoparticles (i.e., Pd, Au, Pt) immobilized into hierarchical meso-/macroporous monoliths were studied for continuous flow C–C couplings [22–24], selective hydrogenations [25–30] and selective oxidation [31], demonstrating the advantages in terms of mass transport and activity (resulting in high productivity and selectivity) with respect to conventional batch systems or packed-bed continuous flow reactors.

Epoxides represent valuable building blocks in organic synthesis due to their reactivity and versatility as intermediates in the fine chemicals, pharmaceuticals and cosmetics industry. Particularly, β-alkoxyalcohols synthesis is traditionally promoted by using homogeneous systems (e.g., tetrafluorborates) [32] and, more recently, heterogeneous acid catalysts such as amberlyst-15 [33], mesoporous aluminosilicate, [34] and sulfated Zr-doped titanoniobate [35]. In previous studies, some of us showed the unexpected Lewis acidity of CuO NPs catalysts obtained by the CH method and their exploitation for the development of bifunctional materials [36–38]. CH-derived CuO/SiO_2 catalyst (12 wt.% Cu), prepared with a mesoporous chromatographic silica of 580 m^2/g as support (particle diameter 5 μm), was reported as an effective acid catalyst able to promote epoxides alcoholysis in batch reactions under very mild conditions [39,40].

Herein, we report for the first time, a simple reproducible approach for the synthesis of Cu-based NPs highly dispersed into hierarchical meso-/macroporous silica monoliths ($CuO@SiO_2$-MN). The novel approach, named flow chemisorption hydrolysis (flow-CH), was derived from the traditional batch CH method that was previously reported to prepare heterogeneous catalysts with a high copper dispersion onto different metal oxides' supports even at high copper loadings [36,41,42]. SEM, TEM, and HAADF-STEM/EDS investigations confirmed the effectiveness of the flow-CH approach to obtain size-controlled CuO nanoparticles homogeneously dispersed into the inorganic monoliths. In this way we are aiming to combine the unique advantages of silica monoliths featuring hierarchical meso-/macroporosity for a continuous flow monolithic system with the possibility to exploit the catalytic properties of CH-derived size-controlled copper-based NPs. The $CuO@SiO_2$-MN was studied in a styrene oxide ring opening reaction under continuous flow-through conditions in the presence of isopropanol. Alcoholysis of styrene oxide gives rise to β–alkoxyalcohols, which are an important class of valuable intermediates. The results were compared with those obtained in more conventional batch reaction conditions using a previously reported CH-derived copper catalyst supported on silica powder [39] and also with grinded $CuO@SiO_2$-MN catalyst. $CuO@SiO_2$-MN in continuous flow showed remarkable activity and stability with negligible Cu leaching. In addition, the activation and re-generation of the catalyst by a mild calcination step (220 °C) was demonstrated.

2. Results and Discussion

2.1. Preparation and Characterization of $CuO@SiO_2$-MN

Among the batch preparation techniques to synthesize supported heterogeneous catalysts, chemisorption-hydrolysis (CH) was revealed to be very effective, combining very high dispersion of the copper phase, and easy preparation steps [36,37]. The CH approach exploits the strong electrostatic interaction between the surface of the support

and the cationic amino-complex of Cu affording, after hydrolysis and calcination steps, heterogeneous Cu-based catalysts containing a highly dispersed CuO phase. Particularly, very small CuO nanoparticles (NPs) with a mean diameter of 3.2 nm were obtained on silica. On the other hand, ten times larger NPs were obtained by using a traditional wet-impregnation method [36,37].

Here, the copper adsorption/deposition was carried out in silica monoliths (0.6 cm diameter, ~3.5 cm length, ~300 mg) featuring 5 µm diameter macropores (V_{macro} ~1 mL/g) and 10 nm diameter mesopores (V_{meso} ~1.2 mL/g, S_{BET} ~700 m^2/g) by using the CH approach in mild flow conditions at room temperature with a custom glass-deposition column. The copper deposition apparatus is composed of an HPLC pump that ensures the circulation of the copper precursor-solution and a deposition column, where the bare silica monolith was arranged (Figure 1). The silica monolith was enclosed by fine sand that keeps it in place, while being inert toward the Cu adsorption. The aqueous $[Cu(NH_3)_4]^{2+}$ solution (pH 9.5) was left in recirculation for 1 h in the apparatus. Differently to other approaches, using pre-formed metal NPs, CH has the great advantage of using a well-soluble Cu cationic complex in water, that can easily flow through the macropores and diffuse into the mesopores of the monolith, thus favoring a highly homogeneous distribution of the resulting CuO NPs after calcination. The copper-loaded monolith is then calcined in air at 350 °C allowing the formation of small CuO NPs entrapped in the porous structure. The detailed procedure is reported below. The high CuO NPs dispersion is crucial to ensure the Lewis acidity of the resulting catalyst. The copper deposition and calcination steps retained the morphology of the parent silica monolith as well as its macroporous network as confirmed by SEM images of CuO@SiO_2-MN (Figure 1). CuO@SiO_2-MN has a homogeneous light blue color indicating a homogeneous dispersion of Cu (Figure 1). The copper dispersion was investigated by SEM-EDS that showed a high spatial homogeneity of the copper across the transverse plane with an atomic ratio Cu/Si of ~0.25 (Figure 2) with some small deviances close to the outer border. Transmission electron microscopy (Figure 3) showed the very homogenous and uniform copper deposition within the monolith, with a very high dispersion of the metal phase and the formation of very small CuO NPs (mean particles size centered at 2.9 nm), similar to what was obtained by the traditional CH method [36]. XRD showed no peaks of CuO confirming the small particle size (<5 nm) of CuO NPs in silica monoliths (Figure S1). Additionally, TPR analysis on fresh CuO@SiO_2-MN (Figure S2) shows a very symmetrical and sharp peak, with a maximum located at a relatively low temperature (about 230 °C). This indicates the presence of a uniform and highly dispersed copper phase, easy to be reduced to metallic Cu [36,37]. The final Cu loading measured by ICP-OES analysis resulted in 8.4 wt.%, in agreement with the amount of Cu precursor used and as expected using the CH method. Nitrogen sorption isotherm at 77 K shows that the CuO@SiO_2-MN catalyst features a specific surface area (S_{BET}) of 315 m^2/g, a mesopore volume of 0.99 mL/g, and mesopore diameter of 15.5 nm. The larger mesopore diameter of CuO@SiO_2-MN in comparison to the one in the initial silica monolith (Figure S3) indicates that a restructuring of the mesopores network has occurred during the 1 h Cu impregnation in basic medium (pH 9.5), resulting in the formation of larger silica NPs of 11–18 nm within the skeleton as observed by TEM (Figure 1), leading to larger mesopore diameter and lower specific surface area. The Cu species are not just deposited on the silica surface but participate in the silica mesopores' formation.

Before proceeding to the catalytic tests, the CuO@SiO_2-MN was clad with a heat-shrinkable Teflon sleeve, along with two glass tubes as terminals, to easily connect the monolith with the in-flow test system [10].

2.2. Catalytic Tests

CH-derived CuO/SiO_2 catalysts were previously reported to effectively promote the alcoholysis of styrene oxide to the corresponding β-alkoxyalcohol, using 2-propanol, both as reagent and solvent in a batch reactor at 60 °C. Under these conditions (styrene oxide concentration of 0.16 M, catalyst amount 20 g/L) a conversion of 100% was reached in

0.75 h with an 83% selectivity for the corresponding β-alkoxyalcohol (Figure 4) [24]. For comparison, the catalytic performance of the CuO@SiO_2-MN was first studied in batches under the same conditions. The CuO@SiO_2-MN monolith was first grinded into particles of ~100–200 µm. This resulted in a conversion of 97% of styrene oxide after 3 h (41% after 1 h and >99.9% after 4 h) and a complete selectivity towards β-alkoxyalcohol (>99.9%) (Figure S4). The reaction over the grinded monolith CuO@SiO_2-MN is slower than the one over CuO/SiO_2 catalyst, which is maybe due to the huge structural difference between the two silica supports and/or external diffusion limitation, due to the large difference in catalyst particle size (5 µm against 100–200 µm) and the different copper loading, but the selectivity over the ground monolith CuO@SiO_2-MN is higher and totally towards β-alkoxyalcohol. CuO@SiO_2-MN reveals the highest selectivity reported for this reaction with a Cu-based catalyst. In the literature, another kind of catalyst, sulfated Zr-doped titanoniobate (25 g/L), was reported to reach 99% yield of β-alkoxyalcohol in 3 h, in batch, at room temperature, with a styrene oxide concentration of 0.50 M in isopropanol [35]. However, no in flow conversion of oxide ring opening was presented. Batch processes need a further separation step to recover the product of interest, in contrast to flow systems.

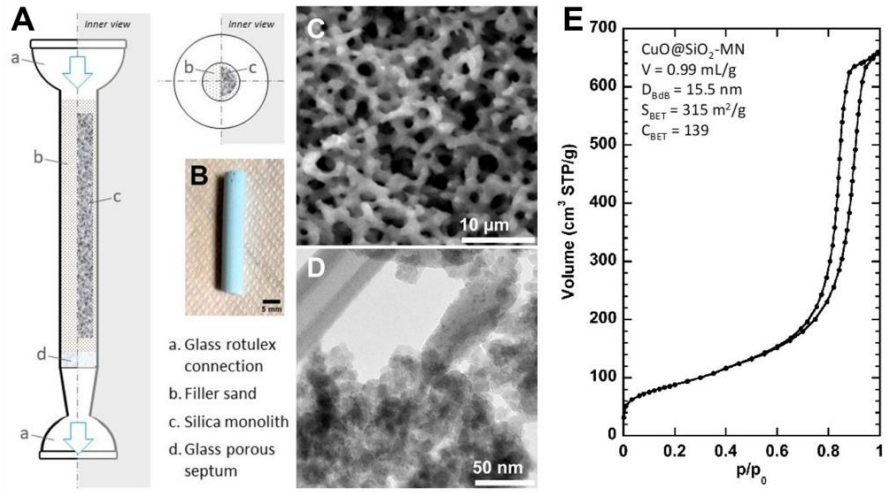

Figure 1. (**A**) Graphical sketch of the set up used for Cu deposition on the silica monolith. (**B**) Picture, (**C**) SEM and (**D**) TEM images and (**E**) N_2 sorption at 77 K of CuO@SiO_2-MN after calcination at 350 °C (pristine catalyst).

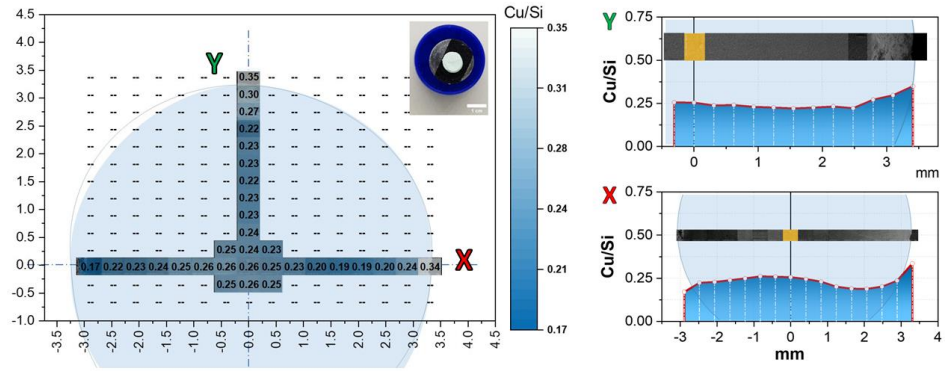

Figure 2. Composite image of SEM micrographs of CuO@SiO_2-MN and related EDS analysis. The picture shows the SEM-EDS analysis area/micrograph recorded by single frames of 291.10 µm × 388.22 µm across the sample section. Full EDS spectra and calculated atomic% for Cu and Si were recorded for each frame. In the picture, we report the Cu/Si signal ratio to follow the sample morphology and to smooth working distance changes. In the inset, a picture of the sample section mounted onto the SEM pin for SEM-EDX analysis.

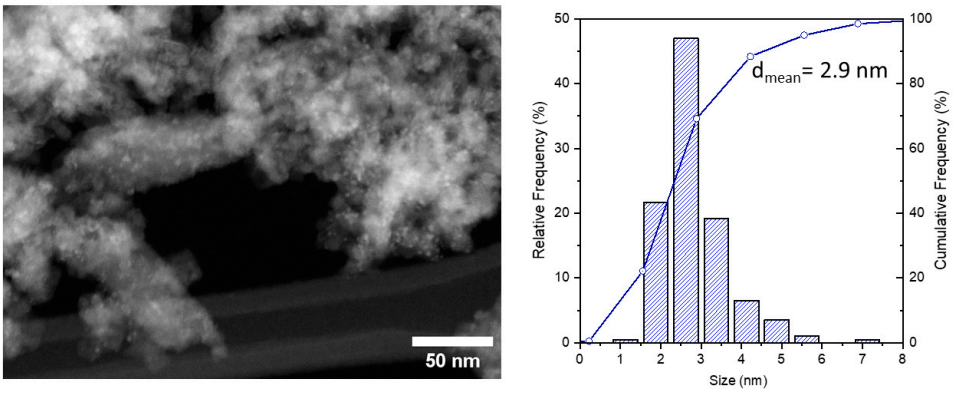

Figure 3. Representative HAADF-STEM micrograph of the fresh CuO@SiO_2-MN and related histogram of particle size distribution.

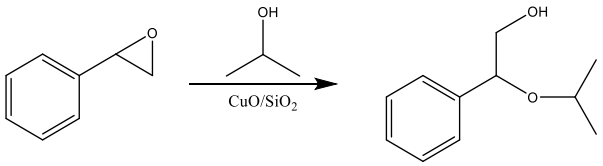

Figure 4. Styrene oxide alcoholysis with 2-propanol.

Considering this promising result, the epoxide ring opening reaction was performed in continuous flow using the CuO@SiO_2-MN in one piece (0.6 cm diameter, 3.5 cm length, ~330 mg, 0.43 mmol Cu). The initial screening was performed by changing the styrene oxide concentration and the flow rate (Figure 5). Particularly, four different styrene oxide concentrations were investigated (i.e., 0.027, 0.035, 0.052 and 0.087 M) and different reaction flow rates, were explored (from 0.1 to 1.0 mL/min) for a total of about 12 h under flow conditions. The contact time was calculated by dividing the monolith volume by the flow rate. The styrene oxide conversion increases by increasing the contact time and by decreasing the epoxide concentrations (Figure 5). The highest conversions were obtained using a 0.027 M and 0.035 M styrene oxide solution (i.e., Conv. $\geq$99.9% and 97%, respectively) for the same contact time of 9.9 min (Figure 5). The regioselectivity (>99.9%) was complete towards the β-alkoxyalcohol and was stable with time under flow for all the studied conditions.

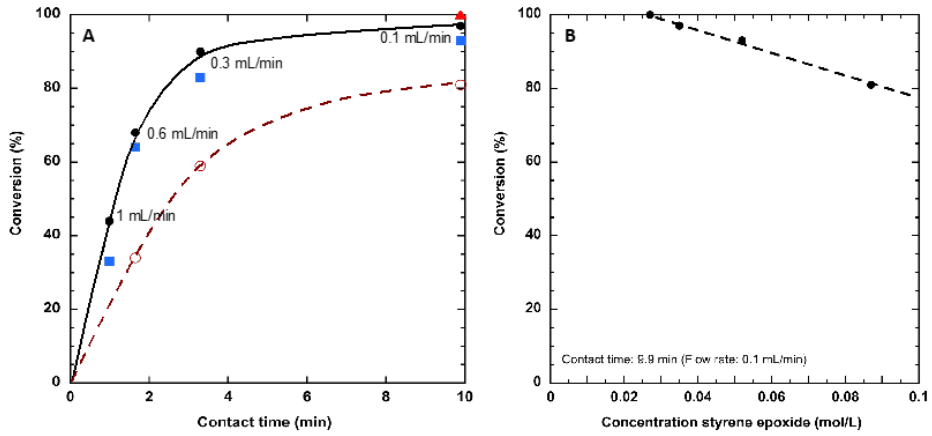

Figure 5. Styrene oxide alcoholysis reaction with CuO@SiO_2-MN in continuous flow. (**A**) conversion as a function of contact time for different styrene oxide concentrations: (red triangle) 0.027 M, (black points) 0.035 M, (blue square) 0.052 M, (red circle) 0.087 M; (**B**) conversion as a function of styrene concentration for the same contact time of 9.9 min (same flow rate of 0.1 mL/min).

In terms of specific activity (SA, SA = mmol styrene oxide converted × mmol Cu^{-1} × h^{-1}), comparable results (i.e., ca. 3.5 h^{-1}) were obtained with similar styrene oxide conversion by using different flow rates and styrene oxide concentration: for 0.035 M, 1 mL/min, 44% conversion, SA 3.0 h^{-1}; for 0.052 M, 1 mL/min, 33% conversion, SA 3.4 h^{-1}; for 0.087 M, 0.6 mL/min, 34% conversion, SA 3.5 h^{-1}. Noteworthy, the SA of the CuO@SiO_2-MN in continuous-flow conditions was sensibly higher than that observed with the same grinded catalyst under batch conditions, calculated at similar conversions (3.0–3.5 h^{-1} vs. 2.7 h^{-1}). Moreover, it is important to note that the reactions led to a complete regioselectivity (>99.9%) towards the β-alkoxyalcohol for all tested conditions.

The concentration of 0.035 M of styrene oxide and 0.1 mL/min flow rate (contact time 9.9 min), were selected to study the recyclability/durability of the CuO@SiO_2-MN catalyst. With this aim, the same reactor was tested for 43 h in continuous-flow, monitoring the efficiency of the CuO@SiO_2-MN catalyst (Figure 6).

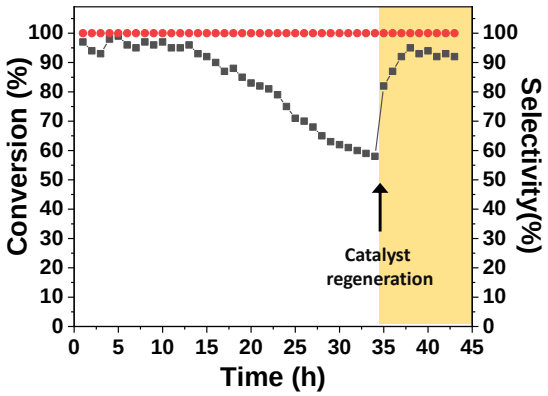

Figure 6. Continuous-flow catalytic reaction using CuO@SiO_2-MN. Reaction conditions: T = 60 °C, air, styrene oxide 0.035 M, flow rate 0.1 mL/min: (black squares) conversion, (red circles) selectivity for β-alkoxy alcohol.

During the first 13 h an essentially complete conversion of styrene oxide (95–98%) and the selective formation of the corresponding β-alkoxy alcohol were attained. After 14 h a gradual constant decrease in catalytic efficiency was observed and after 34 h the conversion of styrene oxide was 58%. This decrease is in agreement with the one observed in the recycling test for the batch system [39], but it is worth noting that, unlike what was previously observed in the batch reaction, a complete regioselectivity was maintained.

In order to thoroughly investigate the possible role of Cu leaching on the observed catalyst deactivation, the Cu contents of the reaction mixtures collected during the first 34 h were analyzed by ICP-OES. A maximum amount of Cu in solution of 1.0 ppm was detected corresponding to less than 0.6 wt.% of the initial Cu content measured into the monolith. Moreover, to support the heterogenous nature of the catalyst, a portion of the reaction mixture collected after 34 h (showing a styrene oxide conversion of 58%) was maintained at 60 °C under stirring. After 2 h under reaction conditions no further conversion was observed. On the other hand, the partial deactivation of the catalyst could be due to the presence of residual carbon species blocking the copper active sites. To validate this hypothesis, after 34 h under reaction conditions, the CuO@SiO_2-MN device was washed with 2-propanol, dried and treated at 220 °C for 3 h. After this treatment, a significant increase in conversion was observed (95%, after 38 h) and the catalyst showed a good stability, at least for the further 7 h under reaction conditions (92%, after 43 h). Summarizing, the catalyst showed productivity (24.7 mmol β-alkoxyalcohol/mmol Cu; space time yield = 0.18 mmol β-alkoxyalcohol/(h × cm^3)) and selectivity higher than the previously reported Cu on silica catalyst (17.3 mmol β-alkoxyalcohol/mmol Cu by using ethanol instead of 2-propanol). TEM images on spent catalyst show only a slight aggregation of the CuO NPs, with a mean size that moved from 2.9 to 3.6 nm (Figure 7), excluding a major role of the CuO NPs size increase on the catalyst deactivation. In

agreement with TEM results, no CuO peaks are observed in the XRD pattern of spent catalyst confirming the small size of CuO NPs (<5 nm), even after the catalytic tests (Figure S1). The TPR profile of the spent catalyst points out a reduction temperature (with a maximum around 230 °C), very similar to the fresh sample, while a limited broadening of the peak agrees with the slight aggregation of CuO NPs (Figure S2) observed by TEM. On the other hand, thermogravimetric analysis (TGA) under an oxygen atmosphere, of spent catalyst (Figure S5) confirmed the presence of adsorbed organic species (<4 wt.%) at the surface of CuO NPs, which are decomposed between 100–700 °C (less than 1 wt.% at 220 °C).

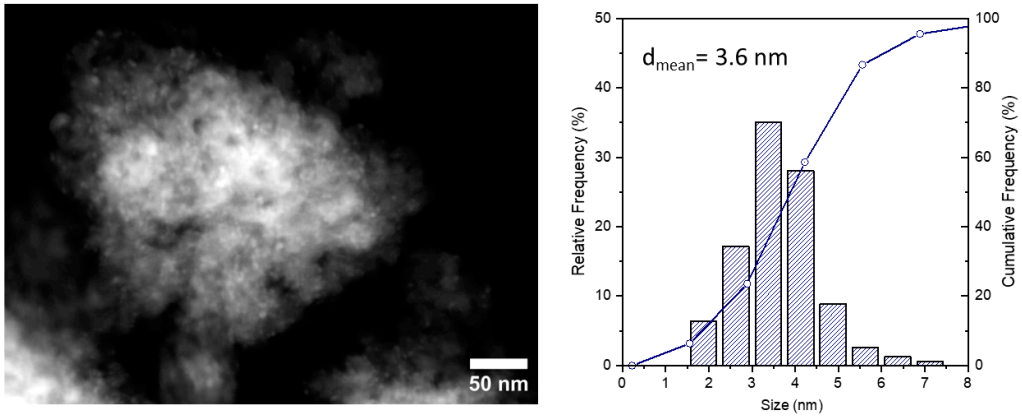

Figure 7. Representative STEM micrographs of CuO@SiO_2-MN after 43 h of catalysis under flow and related particle size distribution.

3. Materials and Methods

3.1. General

TEM (Transmission Electron Microscopy) and STEM (Scanning TEM) characterization were performed on a ZEISS LIBRA200FE (Oberkochen, Germany). Samples were gently smashed in an agate mortar, suspended in isopropyl alcohol, sonicated for 15 min, and dropped onto a lacey-carbon-coated Cu TEM grid. Specimens were dried overnight before analysis. SEM (Scanning Electron Microscopy) analyses were performed by a Philips XL30 ESEM (Amsterdam, The Netherlands) working in low vacuum mode 0.8 torr–15 kV. The monolith was cut in a small cylindrical pellet, keeping the general morphology, and mounted onto an SEM pin with carbon tape. SEM-EDS (Energy-dispersive X-ray spectroscopy) was performed by an EDAX-Element probe.

Inductively coupled plasma-optical emission (ICP-OES) analysis was carried out by inductively coupled plasma-optical emission spectroscopy (ICP-OES) (Perkin Elmer Optima 8000, Waltham, MA, USA) and an external calibration methodology. For ICP-OES, a small amount (5 mg) of CuO@SiO_2-MN was heated in a porcelain crucible in the presence of aqua regia (2 mL) for four times, dissolving the solid residue in 0.5 M aqueous HCl. The solution was then diluted to 100 mL. The limit of detection (lod) calculated for copper was 0.01 ppm.

The specific surface area (S_{BET}) of CuO@SiO_2-MN was measured after evacuation of the sample (ca. 100 mg) at 200 °C for 2 h, by collecting N_2 adsorption/desorption isotherms at −196 °C using a Micromeritics ASAP2020 surface area analyzer (Norcross, GA, USA). Mesopore diameters were determined from the desorption isotherm with the Broekhoff and De Boer method, previously shown as more accurate for silica materials [43].

X-ray diffraction (XRD) was performed on a Philips X'Pert device (Cu Kα radiation λ = 1.54060 Å) in the range 2θ = 10–70° with a 0.0170° angular step and counting time of 40 s per step.

Temperature-programmed reduction (TPR) analysis was performed with a modified version of the Pulse Chemisorb 2700 apparatus from Micromeritics. Catalysts (samples containing ca. 1 mg of Cu) were diluted with quartz, calcined at 350 °C under O_2 (40 mL/min),

and then reduced at 8 °C/min under a flow (15 mL/min) of an 8% H_2/Ar mixture. The H_2 consumption was detected by a thermal conductivity detector (TCD).

3.2. Monolith Synthesis

SiO_2 monoliths were synthesized from tetraethylorthosilicate (TEOS, Aldrich, St. Louis, MO, USA) in the presence of polyethylene oxide (PEO 20 kDa, Sigma, St. Louis, MO, USA) in a nitric acid solution (molar ratio: 1 Si:0.60 EO:0.26 HNO_3:14.21 H_2O), followed by a basic post-treatment with NH_3 aqueous solution 0.1 M at 40 °C for 24 h, as reported earlier [12]. The monoliths are then calcined at 550 °C for 8 h to remove the polymers. The resulting monoliths feature a macropore diameter of 5 µm and mesopore diameter of 10 nm.

3.3. CuO NP Deposition into SiO_2 Monolith

First, the monolith (240 mg) was placed into a tubular glass deposition reactor column equipped with a porous septum from one side. The empty space between the reactor walls and the monolith was filled with sand and the upper junction of the glass reactor was connected to an HPLC pump through a stainless steel tube. The $[Cu(NH_3)_4]^{2+}$ solution was prepared by dissolving 5 g of $Cu(NO_3)_2 \cdot 3H_2O$ in 30 mL of H_2O and then adding NH_3 ($\geq$25% in water) until pH = 9.5. This solution was recirculated (10 mL/min) through the monolith for 1 h for the chemisorption step. After this the monolith was washed with 500 mL of water, extracted from the reactor and calcinated in air at 350 °C for 4 h. After the calcination the CuO@SiO_2-MN and two glass tubes (4–5 cm) were clad with a heat shrinkable Teflon gain (FEP AWG 6, Castello, France). The Teflon gain was shrunk at 350 °C for 10 min.

3.4. Catalytic Tests

Batch alcoholysis reactions were carried out in a glass reactor using 100 mg of grinded CuO@SiO_2-MN catalyst (0.13 mmol Cu), 0.8 mmol of styrene oxide and 5 mL of 2-propanol (0.16 M styrene oxide) at 60 °C, under N_2 with stirring (1100 rpm) for 2 h. The continuous-flow tests with CuO@SiO_2-MN monoliths (0.6 cm diameter, ~3.5 cm length, mass ~330 mg, ~0.43 mmol Cu) were carried out using a styrene oxide/2-propanol solution (0.027, 0.035 M, 0.052 M, 0.087 M) fed through an HPLC pump at different flow ratios (0.1, 0.3, 0.6 and 1 mL/min) at 60 °C for several hours under air. Before the reaction, the clad CuO@SiO_2-MN was connected from one side to the HPLC pump (through one of the glass tubes—see Sectiob 3.3 CuO NPs deposition over SiO_2 monolith) and, from the other side to a tube for collecting liquid samples.

4. Conclusions

In conclusion, CuO NPs were successfully deposited (8.4 wt.%) over hierarchical meso-/macroporous SiO_2 monoliths using a continuous flow-through protocol based on a CH method, reported for the first time. The approach, named the flow-CH, allowed small NPs (mean diameter 2.8 nm) to be obtained that were highly and homogenously dispersed along the monolith. This technique allows one of the main limitations of these systems to be overcome, as alternative preparation methods based on the deposition of pre-formed NPs suffer from a non-uniform deposition inside monolithic supports. Moreover, the transition between the traditional batch CH method to a flow one is a step up allowing easier applicability and scalability of this catalyst's synthesis, also with packed-bed powder supports. The CuO-based monolith showed high catalytic performances (>99.9% conversion for a contact time of 9.9 min and [styrene oxide] = 0.027 M in isopropanol) under continuous-flow conditions for the selective alcoholysis of styrene oxide with isopropanol towards the corresponding β-alkoxyalcohol, as unique product. Higher performances than previously reported for Cu on silica catalyst in terms of productivity (24.7 mmol β-alkoxyalcohol/mmol Cu; space time yield = 0.18 mmol β-alkoxyalcohol/(h $\times$ cm^3)) and selectivity were achieved. The conversion was stable for 13 h in flow. A very low metal leaching was observed (less than 0.6 wt.% of initial Cu) and the feasibility of extending the

catalyst's lifetime after 13 h in flow by re-generating the catalyst by mild thermal treatment (220 °C) was demonstrated.

Furthermore, the flow-CH approach can be easily extended to other metals for the preparation of uniform metal-based monoliths, with small nanoparticles. Indeed, it can be easily extended to metals that form amino-complexes (e.g., Ni, Pd, Pt, Ru), to obtain more uniform and well dispersed metal-monolith materials. For that reason, the application of the CH method to monoliths, represents an advancement in the effective utilization of these systems. These CuO-based monoliths should also be a great opportunity to develop other kinds continuous flow reactions that are commonly carried out using CuO/SiO_2 catalysts in batch [40] such as Friedel–Crafts acylation and alkylation, and selective hydrogenation and dehydrogenation after a pre-reduction treatment.

Supplementary Materials: The following supporting information can be downloaded at: https://www.mdpi.com/article/10.3390/catal13020341/s1, Figure S1: XRD pattern of (black) parent silica monolith (SiO_2-MN), (blue) CuO@SiO_2-MN monolith and (grey) CuO@SiO_2-MN monolith after 43 h of catalysis; Figure S2: TPR of (blue) CuO@SiO_2-MN monolith and (grey) CuO@SiO_2-MN monolith after 43 h of catalysis; Figure S3: Nitrogen sorption isotherms at 77 K of parent silica monolith (SiO_2-MN) and CuO@SiO_2-MN monolith; Figure S4: Conversion of styrene oxide with 2-propanol as a function of time carried out with CuO@SiO_2-MN under batch reaction conditions; Figure S5: TGA analysis of the spent CuO@SiO_2-MN catalyst after 43 h under continuous flow reaction conditions.

Author Contributions: Conceptualization, C.E.; methodology, N.S., F.Z. and N.R.; formal analysis, M.M. and E.P.; monoliths synthesis and characterization, Y.D. and A.G.; investigation, N.S. and M.M.; resources, N.S., M.M. and C.E.; writing—original draft preparation, N.S., M.M. and C.E.; writing—review and editing, F.Z., N.R., E.P. and A.G. All authors have read and agreed to the published version of the manuscript.

Funding: Y.D. and A.G. thanks ANR French agency for funding, Project ANR-TAMTAM N° ANR-15-CE08-0008-01.

Data Availability Statement: Not applicable.

Acknowledgments: Authors thank Marco Fabbiani for XRD measurements.

Conflicts of Interest: The authors declare no conflict of interest.

References

1. Hommes, A.; Heeres, H.J.; Yue, J. Catalytic Transformation of Biomass Derivatives to Value-Added Chemicals and Fuels in Continuous Flow Microreactors. *ChemCatChem* **2019**, *11*, 4671–4708. [CrossRef]
2. Wiles, C.; Watts, P. Continuous Flow Reactors: A Perspective. *Green Chem.* **2012**, *14*, 38–54. [CrossRef]
3. Noêl, T.; Buchwald, S.L. Cross-Coupling in Flow. *Chem. Soc. Rev.* **2011**, *40*, 5010–5029. [CrossRef]
4. Su, B.L.; Sanchez, C.; Yang, X.Y. *Hierarchically Structured Porous Materials: From Nanoscience to Catalysis, Separation, Optics, Energy, and Life Science*; John Wiley & Sons: New York, NY, USA, 2011; ISBN 9783527327881.
5. Feinle, A.; Elsaesser, M.S.; Hüsing, N. Sol-Gel Synthesis of Monolithic Materials with Hierarchical Porosity. *Chem. Soc. Rev.* **2016**, *45*, 3377–3399. [CrossRef]
6. Munirathinam, R.; Huskens, J.; Verboom, W. Supported Catalysis in Continuous-Flow Microreactors. *Adv. Synth. Catal.* **2015**, *357*, 1093–1123. [CrossRef]
7. Govender, S.; Friedrich, H.B. Monoliths: A Review of the Basics, Preparation Methods and Their Relevance to Oxidation. *Catalysts* **2017**, *7*, 62. [CrossRef]
8. Haas, C.P.; Müllner, T.; Kohns, R.; Enke, D.; Tallarek, U. High-Performance Monoliths in Heterogeneous Catalysis with Single-Phase Liquid Flow. *React. Chem. Eng.* **2017**, *2*, 498–511. [CrossRef]
9. Poupart, R.; Le Droumaguet, B.; Guerrouache, M.; Carbonnier, B. Copper Nanoparticles Supported on Permeable Monolith with Carboxylic Acid Surface Functionality: Stability and Catalytic Properties under Reductive Conditions. *Mater. Chem. Phys.* **2015**, *163*, 446–452. [CrossRef]
10. Galarneau, A.; Sachse, A.; Said, B.; Pelisson, C.H.; Boscaro, P.; Brun, N.; Courtheoux, L.; Olivi-Tran, N.; Coasne, B.; Fajula, F. Hierarchical Porous Silica Monoliths: A Novel Class of Microreactors for Process Intensification in Catalysis and Adsorption. *Comptes Rendus Chim.* **2016**, *19*, 231–247. [CrossRef]
11. Sachse, A.; Galarneau, A.; Fajula, F.; Di Renzo, F.; Creux, P.; Coq, B. Functional Silica Monoliths with Hierarchical Uniform Porosity as Continuous Flow Catalytic Reactors. *Microporous Mesoporous Mater.* **2011**, *140*, 58–68. [CrossRef]

12. Didi, Y.; Said, B.; Cacciaguerra, T.; Nguyen, K.L.; Wernert, V.; Denoyel, R.; Cot, D.; Sebai, W.; Belleville, M.P.; Sanchez-Marcano, J.; et al. Synthesis of Binderless FAU-X (13X) Monoliths with Hierarchical Porosity. *Microporous Mesoporous Mater.* **2019**, *281*, 57–65. [CrossRef]
13. Sebai, W.; Ahmad, S.; Belleville, M.-P.; Boccheciampe, A.; Chaurand, P.; Levard, C.; Brun, N.; Galarneau, A.; Sanchez-Marcano, J. Biocatalytic Elimination of Pharmaceutics Found in Water With Hierarchical Silica Monoliths in Continuous Flow. *Front. Chem. Eng.* **2022**, *4*, 823877. [CrossRef]
14. Ou, J.; Liu, Z.; Wang, H.; Lin, H.; Dong, J.; Zou, H. Recent Development of Hybrid Organic-Silica Monolithic Columns in CEC and Capillary LC. *Electrophoresis* **2015**, *36*, 62–75. [CrossRef] [PubMed]
15. He, P.; Haswell, S.J.; Fletcher, P.D.I.; Kelly, S.M.; Mansfield, A. Scaling up of Continuous-Flow, Microwave-Assisted, Organic Reactions by Varying the Size of Pd-Functionalized Catalytic Monoliths. *Beilstein J. Org. Chem.* **2011**, *7*, 1150–1157. [CrossRef]
16. El Kadib, A.; Chimenton, R.; Sachse, A.; Fajula, F.; Galarneau, A.; Coq, B. Functionalized Inorganic Monolithic Microreactors for High Productivity in Fine Chemicals Catalytic Synthesis. *Angew. Chemie-Int. Ed.* **2009**, *48*, 4969–4972. [CrossRef]
17. Sachse, A.; Galarneau, A.; Coq, B.; Fajula, F. Monolithic Flow Microreactors Improve Fine Chemicals Synthesis. *N. J. Chem.* **2011**, *35*, 259–264. [CrossRef]
18. Song, G.Q.; Lu, Y.X.; Zhang, Q.; Wang, F.; Ma, X.K.; Huang, X.F.; Zhang, Z.H. Porous Cu-BTC Silica Monoliths as Efficient Heterogeneous Catalysts for the Selective Oxidation of Alkylbenzenes. *RSC Adv.* **2014**, *4*, 30221–30224. [CrossRef]
19. Kim, S.H.; Shin, C.K.; Ahn, C.H.; Kim, G.J. Syntheses and Application of Silica Monolith with Bimodal Meso/Macroscopic Pore Structure. *J. Porous Mater.* **2006**, *13*, 201–205. [CrossRef]
20. Ciemięga, A.; Maresz, K.; Malinowski, J.J.; Mrowiec-Białoń, J. Continuous-Flow Monolithic Silica Microreactors with Arenesulphonic Acid Groups: Structure–Catalytic Activity Relationships. *Catalysts* **2017**, *7*, 255. [CrossRef]
21. Sachse, A.; Ameloot, R.; Coq, B.; Fajula, F.; Coasne, B.; De Vos, D.; Galarneau, A. In Situ Synthesis of Cu–BTC (HKUST-1) in Macro-/Mesoporous Silica Monoliths for Continuous Flow Catalysis. *Chem. Commun.* **2012**, *48*, 4749–4751. [CrossRef]
22. Wang, G.; Kundu, D.; Uyama, H. One-Pot Fabrication of Palladium Nanoparticles Captured in Mesoporous Polymeric Monoliths and Their Catalytic Application in C-C Coupling Reactions. *J. Colloid Interface Sci.* **2015**, *451*, 184–188. [CrossRef] [PubMed]
23. Jumde, R.P.; Marelli, M.; Scotti, N.; Mandoli, A.; Psaro, R.; Evangelisti, C. Ultrafine Palladium Nanoparticles Immobilized into Poly(4-Vinylpyridine)-Based Porous Monolith for Continuous-Flow Mizoroki-Heck Reaction. *J. Mol. Catal. A Chem.* **2016**, *414*, 55–61. [CrossRef]
24. Moitra, N.; Matsushima, A.; Kamei, T.; Kanamori, K.; Ikuhara, Y.H.; Gao, X.; Takeda, K.; Zhu, Y.; Nakanishi, K.; Shimada, T. A New Hierarchically Porous Pd@HSQ Monolithic Catalyst for Mizoroki-Heck Cross-Coupling Reactions. *N. J. Chem.* **2014**, *38*, 1144–1149. [CrossRef]
25. Pélisson, C.H.; Nakanishi, T.; Zhu, Y.; Morisato, K.; Kamei, T.; Maeno, A.; Kaji, H.; Muroyama, S.; Tafu, M.; Kanamori, K.; et al. Grafted Polymethylhydrosiloxane on Hierarchically Porous Silica Monoliths: A New Path to Monolith-Supported Palladium Nanoparticles for Continuous Flow Catalysis Applications. *ACS Appl. Mater. Interfaces* **2017**, *9*, 406–412. [CrossRef] [PubMed]
26. Liguori, F.; Barbaro, P.; Said, B.; Galarneau, A.; Santo, V.D.; Passaglia, E.; Feis, A. Unconventional Pd@Sulfonated Silica Monoliths Catalysts for Selective Partial Hydrogenation Reactions under Continuous Flow. *ChemCatChem* **2017**, *9*, 3245–3258. [CrossRef]
27. Linares, N.; Hartmann, S.; Galarneau, A.; Barbaro, P. Continuous Partial Hydrogenation Reactions by Pd@unconventional Bimodal Porous Titania Monolith Catalysts. *ACS Catal.* **2012**, *2*, 2194–2198. [CrossRef]
28. Troncoso, F.D.; Tonetto, G.M. Highly Stable Platinum Monolith Catalyst for the Hydrogenation of Vegetable Oil. *Chem. Eng. Process.-Process Intensif.* **2022**, *170*, 108669. [CrossRef]
29. Moitra, N.; Kanamori, K.; Ikuhara, Y.H.; Gao, X.; Zhu, Y.; Hasegawa, G.; Takeda, K.; Shimada, T.; Nakanishi, K. Reduction on Reactive Pore Surfaces as a Versatile Approach to Synthesize Monolith-Supported Metal Alloy Nanoparticles and Their Catalytic Applications. *J. Mater. Chem. A* **2014**, *2*, 12535–12544. [CrossRef]
30. Russell, M.G.; Veryser, C.; Hunter, J.F.; Beingessner, R.L.; Jamison, T.F. Monolithic Silica Support for Immobilized Catalysis in Continuous Flow. *Adv. Synth. Catal.* **2020**, *362*, 314–319. [CrossRef]
31. Alotaibi, M.T.; Taylor, M.J.; Liu, D.; Beaumont, S.K.; Kyriakou, G. Selective Oxidation of Cyclohexene through Gold Functionalized Silica Monolith Microreactors. *Surf. Sci.* **2016**, *646*, 179–185. [CrossRef]
32. Barluenga, J.; Vàzquez-Villa, H.; Ballesteros, A.; Gonza, M. Copper (II) Tetrafluoroborate Catalyzed Ring-Opening Reaction of Epoxides With. *Org. Lett.* **2002**, *4*, 2817–2819. [CrossRef] [PubMed]
33. Liu, Y.H.; Liu, Q.S.; Zhang, Z.H. Amberlyst-15 as a New and Reusable Catalyst for Regioselective Ring-Opening Reactions of Epoxides to β-Alkoxy Alcohols. *J. Mol. Catal. A Chem.* **2008**, *296*, 42–46. [CrossRef]
34. Robinson, M.W.C.; Buckle, R.; Mabbett, I.; Grant, G.M.; Graham, A.E. Mesoporous Aluminosilicate Promoted Alcoholysis of Epoxides. *Tetrahedron Lett.* **2007**, *48*, 4723–4725. [CrossRef]
35. Zhang, L.; Hu, C.; Mei, W.; Zhang, J.; Cheng, L.; Xue, N.; Ding, W.; Chen, J.; Hou, W. Highly Efficient Sulfated Zr-Doped Titanoniobate Nanoplates for the Alcoholysis of Styrene Epoxide at Room Temperature. *Appl. Surf. Sci.* **2015**, *357*, 1951–1957. [CrossRef]
36. Zaccheria, F.; Scotti, N.; Marelli, M.; Psaro, R.; Ravasio, N. Unravelling the Properties of Supported Copper Oxide: Can the Particle Size Induce Acidic Behaviour? *Dalt. Trans.* **2013**, *42*, 1319–1328. [CrossRef]

37. Scotti, N.; Dangate, M.; Gervasini, A.; Evangelisti, C.; Ravasio, N.; Zaccheria, F. Unraveling the Role of Low Coordination Sites in a Cu Metal Nanoparticle: A Step toward the Selective Synthesis of Second Generation Biofuels. *ACS Catal.* **2014**, *4*, 2818–2826. [CrossRef]
38. Scotti, N.; Finocchio, E.; Evangelisti, C.; Marelli, M.; Psaro, R.; Ravasio, N.; Zaccheria, F. Some Insight on the Structure/Activity Relationship of Metal Nanoparticles in Cu/SiO_2 Catalysts. *Chin. J. Catal.* **2019**, *40*, 1788–1794. [CrossRef]
39. Zaccheria, F.; Santoro, F.; Psaro, R.; Ravasio, N. CuO/SiO_2: A Simple and Efficient Solid Acid Catalyst for Epoxide Ring Opening. *Green Chem.* **2011**, *13*, 545–548. [CrossRef]
40. Zaccheria, F.; Shaikh, N.I.; Scotti, N.; Psaro, R.; Ravasio, N. New Concepts in Solid Acid Catalysis: Some Opportunities Offered by Dispersed Copper Oxide. *Top. Catal.* **2014**, *57*, 1085–1093. [CrossRef]
41. Scotti, N.; Zaccheria, F.; Evangelisti, C.; Psaro, R.; Ravasio, N. Dehydrogenative Coupling Promoted by Copper Catalysts: A Way to Optimise and Upgrade Bio-Alcohols. *Catal. Sci. Technol.* **2017**, *7*, 1386–1393. [CrossRef]
42. Scotti, N.; Ravasio, N.; Zaccheria, F.; Psaro, R.; Evangelisti, C. Epoxidation of Alkenes through Oxygen Activation over a Bifunctional CuO/Al_2O_3 Catalyst. *Chem. Commun.* **2013**, *49*, 1957–1959. [CrossRef] [PubMed]
43. Galarneau, A.; Desplantier, D.; Dutartre, R.; Di Renzo, F. Micelle-Templated Silicates as a Test Bed for Methods of Mesopore Size Evaluation. *Microporous Mesoporous Mater.* **1999**, *27*, 297–308. [CrossRef]